PRAMANA
— journal of
physics



Vol. 72, No. 6
June 2009
pp. 927–937

# Role of asymmetries in the chaotic dynamics of the double-well Duffing oscillator

V RAVICHANDRAN[1], S JEYAKUMARI[1], V CHINNATHAMBI[1], S RAJASEKAR[2,*] and M A F SANJUÁN[3]

[1]Department of Physics, Sri K.G.S. Arts College, Srivaikuntam 628 619, India
[2]School of Physics, Bharathidasan University, Tiruchirapalli 620 024, India
[3]Departamento de Física, Universidad Rey Juan Carlos, Tulipán s/n, 28933 Móstoles, Madrid, Spain
*Corresponding author. E-mail: rajasekar@cnld.bdu.ac.in

MS received 4 February 2009; accepted 10 April 2009

**Abstract.** Duffing oscillator driven by a periodic force with three different forms of asymmetrical double-well potentials is considered. Three forms of asymmetry are introduced by varying the depth of the left-well alone, location of the minimum of the left-well alone and above both the potentials. Applying the Melnikov method, the threshold condition for the occurrence of horseshoe chaos is obtained. The parameter space has regions where transverse intersections of stable and unstable parts of left-well homoclinic orbits alone and right-well orbits alone occur which are not found in the symmetrical system. The analytical predictions are verified by numerical simulation. For a certain range of values of the control parameters there is no attractor in the left-well or in the right-well.

**Keywords.** Asymmetrical double-well Duffing oscillator; Melnikov method; horseshoe chaos; asymptotic chaos.

**PACS Nos 05.45.Pq; 05.45.Gg; 02.30.Hq; 02.60.Cb**

## 1. Introduction

Various bifurcations and chaotic dynamics have been investigated in the forced and damped Duffing oscillator [1–3]

$$\ddot{x} + d\dot{x} + \omega_0^2 x + \beta x^3 = f \sin \omega t. \tag{1}$$

The Duffing oscillator has served as a prototype model for various physical and engineering problems. Dynamics of certain nonlinear asymmetrical systems has also been considered in the past. However, the role of variation of differences in the depths of the wells and widths of the wells are yet to be studied in detail on various nonlinear phenomena. Such studies will help us not only to understand the role of asymmetry in the depth and width of the two wells but also to have different types of orbits in different wells.

Asymmetry can be introduced in different ways in the system (1). For instance, addition of constant bias [4–6], quadratic nonlinear term $x^2$ [4,7–9], variable shape parametric perturbation [10,11], replacing cubic nonlinearity by the quadratic nonlinear term [12–14] and asymmetrical periodic driving force [15] have physical significance and represent real physical systems in different disciplines. In the presence of such symmetry breaking perturbations, the occurrence of homoclinic bifurcation, structure of strange attractors, hysteresis jump, routes to chaos, basin boundary structure and escape dynamics have been investigated in the Duffing oscillator. In addition, the effect of variable shape forces [16,17], different types of periodic forces [15] and nonlinear damping [18,19] have also been analysed.

In the present work we wish to study the role of asymmetries, particularly the difference in the depths and widths of the two wells, in the chaotic dynamics of the linearly damped Duffing oscillator driven by the external force $f \sin \omega t$. We consider three different double-well asymmetrical potentials $V_1$, $V_2$ and $V_3$ given by

$$V_i(x) = \begin{cases} -\frac{1}{2}x^2 + \frac{1}{4}\beta x^4, & x \geq 0 \\ -\frac{1}{2}A_i x^2 + \frac{1}{4}B_i \beta x^4, & x < 0 \end{cases}, \tag{2}$$

where $i = 1, 2, 3$, $A_1 = B_1 = \alpha$, $A_2 = 1/\alpha^2$, $B_2 = A_2^2$, $A_3 = 1$, $B_3 = 1/\alpha^2$ and $\alpha$, $\beta > 0$. For $\alpha \neq 1$, the three potentials $V_1$–$V_3$ have distinct characteristic features. The right-well of them is independent of the asymmetry parameter $\alpha$. The shape of the left-well alone can be changed by varying the parameter $\alpha$. The parameter $\alpha$ induces asymmetry in the potentials (2) in different forms. In $V_1$, $V_2$ and $V_3$ the depth of the left-well alone, the location of the local minimum of the left-well alone and both the depth and the local minimum of the left-well respectively can be varied by the control parameter $\alpha$ by keeping the shape of the right-well unchanged. Figure 1 depicts the effect of asymmetry parameter $\alpha$ on the three potentials for $\beta = 1$.

The potentials $V_1$, $V_2$ and $V_3$ can be experimentally realizable by applying suitable electric or magnetic fields in the region $x < 0$ of the physical systems represented by the symmetrical double-well Duffing oscillator [2,20]. For example, in the experiments with the double-well system of submicron Bi wires change in the depth of one well is produced by varying the applied magnetic field in the region $x < 0$ [21,22]. A double-well potential with the depth of one well larger than that of the other well is observed to be an appropriate model of auditory nerve fibre response [2]. Stochastic resonance in the quantum version of a system with the potential $V_1$ has been studied [23].

The main objective of the present paper is to examine both analytically, using the Melnikov method [2,24], and numerically, the role of depth and location of the local minimum of the left-well on the occurrence of homoclinic and asymptotic chaos. We are interested in the prediction of horseshoe chaos since it is considered as an important source of structural instability of nonlinear systems and the threshold curve for its occurrence in the parameter space indicates regions where dramatic structural changes occur. The Melnikov method gives a function, involving all the parameters of the system, which measures the distance between the stable and unstable manifolds of the saddle. The existence of simple zeros and change in the sign of the Melnikov function at some time $t_0$ imply the occurrence of horseshoe chaos. Using the Melnikov method we analyse the role of the asymmetry parameter

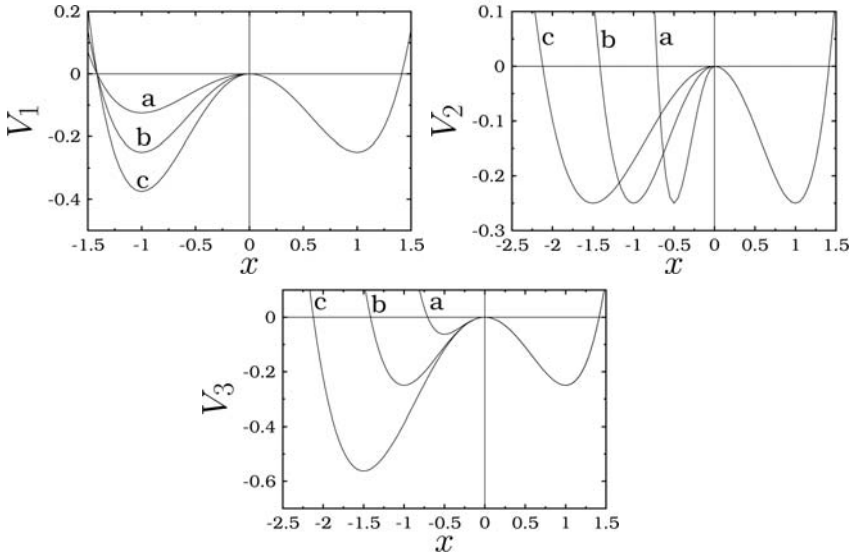


**Figure 1.** The potentials $V_1$, $V_2$ and $V_3$ for three values of $\alpha$ and $\beta = 1$. In all the subplots the potential curves a, b and c correspond to $\alpha = 0.5$, 1 and 1.5 respectively.

$\alpha$ on the onset of horseshoe chaos in the left-well and right-well. Then we carry out numerical study on the onset of asymptotic chaos and bifurcation phenomenon.

As a result of our investigations, we have found certain interesting and nontrivial results. The three kinds of asymmetries lead to the onset of horseshoe chaos and bifurcation phenomenon at different values of the control parameters in the two wells. In the symmetrical double-well system the Melnikov threshold curve (at which the Melnikov function becomes zero) divides the parameter space into two regions. Below the curve the stable and unstable manifolds of the saddle in $x < 0$ and $x > 0$ are well separated and no horseshoe chaos occurs. In this region the system shows regular behaviour. Above the threshold curve transverse intersections of the stable and unstable manifolds of the saddle in $x < 0$ and $x > 0$ occurs. Near the threshold curve the onset of asymptotic chaos or transient chaos is expected. In the asymmetrical systems two additional regions where intersections of the manifolds in $x < 0$ alone and in $x > 0$ alone occur do also exist. In the symmetrical system two types of motion (regular or chaotic) occurs: (i) Two coexisting stable orbits, one confined to $x < 0$ and another confined to $x > 0$. These two orbits undergo bifurcations at the same value of the control parameter. (ii) Cross-well orbit traversing both the regions, $x < 0$ and $x > 0$. The three asymmetries considered in our analysis do not alter the dynamics confined to the region $x > 0$. They alter the bifurcation scenario of the orbits confined to the region $x < 0$. Further, for a range of control parameters we observed no attractors confined to $x < 0$ or $x > 0$.

The plan of the paper is as follows: In §2, we obtain the Melnikov function in the presence of linear damping and periodic forcing ($f \sin \omega t$) and determine the threshold condition for horseshoe chaos. Next, we study the threshold curve in $(\alpha, f)$ and $(f, \omega)$ parameter spaces where $f$ and $\omega$ are the amplitude and the

angular frequency of the periodic force respectively. Interestingly, for a fixed value of $\alpha$, $\alpha \neq 1$, onset of homoclinic bifurcation in the left-well and the right-well occur at different values of the parameters. In §3, analytical predictions are verified by numerically computing the stable and unstable manifolds of the saddle and also by comparing the Melnikov threshold value with the onset of asymptotic chaos or transient chaos. Finally, §4 contains conclusion.

## 2. Threshold curves for homoclinic intersections in $(\alpha, f)$ and $(f, \omega)$ planes

The equations of motion of the systems corresponding to the potentials $V_1$–$V_3$ with the addition of a linear damping term $\mathrm{d}\dot{x}$ and the external periodic force $f \sin \omega t$ are given by

$$\dot{x} = y, \tag{3a}$$

$$\dot{y} = -\frac{\mathrm{d}V_i}{\mathrm{d}x} + \epsilon \left[-\mathrm{d}y + f \sin \omega t\right], \tag{3b}$$

where $i = 1, 2, 3$. We call the systems with the asymmetrical potentials $V_1$, $V_2$ and $V_3$ as system-1, system-2 and system-3 respectively. The homoclinic orbits of the unperturbed systems ($\epsilon = 0$) with the potentials $V_1$, $V_2$ and $V_3$ are given by

$$x_{i,h}(t) = \begin{cases} x_{i,h}^{+} = \sqrt{2/\beta}\ \mathrm{sech}\ t, & x > 0 \\ x_{i,h}^{-} = -\sqrt{2/\beta}\ \gamma_i\ \mathrm{sech}\ \delta_i t, & x < 0 \end{cases}, \tag{4}$$

where $i = 1, 2, 3$ and $\gamma_1 = 1$, $\gamma_2 = \gamma_3 = \alpha$, $\delta_1 = \alpha$, $\delta_2 = 1/\alpha$ and $\delta_3 = 1$. The part of the homoclinic orbits moving away from the saddle point in the region $x < 0$ and $x > 0$ are termed as unstable manifolds $W_{\mathrm{u}}^{-}$ and $W_{\mathrm{u}}^{+}$ respectively. Similarly, $W_{\mathrm{s}}^{-}$ and $W_{\mathrm{s}}^{+}$ are the stable manifolds approaching the saddle in the regions $x < 0$ and $x > 0$ respectively.

For a system of the form

$$\dot{x} = f_1(x, y), \tag{5a}$$

$$\dot{y} = f_2(x, y) + \epsilon g(x, y, t), \tag{5b}$$

where $g$ is periodic in $t$ with period-$T$, the Melnikov function is given by [2,24]

$$M(t_0) = \int_{-\infty}^{\infty} f_1(X_h(t))[g(X_h(t)), t + t_0]\mathrm{d}t, \tag{6}$$

where $X_h = (x_h, y_h)$ represents homoclinic orbits of the unperturbed systems. For each of the three unperturbed systems, the homoclinic orbits in the left-well and the right-well are different. Therefore, the analytical expression for $M(t_0)$ will be different for $x < 0$ and $x > 0$.

For eq. (3) the Melnikov function is given by

$$M^{\pm}(t_0) = \int_{-\infty}^{\infty} y_h^{\pm}[-\mathrm{d}y_h^{\pm} + f\sin\omega(t+t_0)]\mathrm{d}t, \tag{7}$$

where + and − signs refer to the regions $x > 0$ and $x < 0$ respectively and $y_h^{\pm} = \dot{x}_h^{\pm}$. The function $M^{\pm}(t_0)$ for the three systems are calculated as

$$M^{+}_{1,2,3}(t_0) = M^{+}(t_0) = -A + B\,\mathrm{sech}\; C\,\cos\omega t_0, \tag{8}$$

$$M^{-}_{1}(t_0) = -A\sqrt{\alpha} - \frac{B}{\sqrt{\alpha}}\,\mathrm{sech}(C/\sqrt{\alpha}\,)\,\cos\omega t_0, \tag{9}$$

$$M^{-}_{2}(t_0) = -A\alpha - B\alpha^2\,\mathrm{sech}(C\alpha)\cos\omega t_0, \tag{10}$$

$$M^{-}_{3}(t_0) = -A\alpha^2 - B\alpha\,\mathrm{sech}\; C\cos\omega t_0, \tag{11}$$

where $A = 4d/(3\beta)$, $B = \sqrt{2/\beta}\,f\pi\omega$ and $C = \pi\omega/2$. The parameter $\alpha$ occurs in different forms in the Melnikov functions given by eqs (8)–(11). The intersections of the homoclinic orbits, that is intersections of stable and unstable manifolds, are the necessary conditions for the existence of chaos. Homoclinic bifurcation occurs when $M(t_0)$ has a simple zero and changes sign. The necessary threshold condition on the parameters of the systems for horseshoe chaos can be obtained from eqs (8)–(11). For all the three systems the threshold condition for horseshoe chaos in the right-well is given by $f_M^{+} \geq \sqrt{\beta/2}\,(A/\pi\omega)\cosh C$. We can obtain similar conditions for horseshoe chaos in the left-well for the three systems and denote the threshold values of $f$ as $f_M^{-}$. In general, $f_M^{-} \neq f_M^{+}$ for $\alpha \neq 1$.

The threshold curves for horseshoe chaos can be obtained in the $(f, \alpha)$ parameter plane. We fix $\beta = 1$, $\omega = 1$ and $d = 0.5$. A typical plot of $f_M$ against $\alpha$ is shown in figure 2. The characteristic differences and the similarities of the threshold curves of the three systems are summarized below:

- For systems 1 and 2 the variation of $f_M^{-}$ is nonlinear. For system-3 it varies linearly with $\alpha$.
- The $(f, \alpha)$ plane consists of four distinct regions. In the region $R_1$, intersections of the stable and unstable manifolds of saddle do not occur. Homoclinic intersections occur in both wells in the region $R_2$. In the regions $R_3$ and $R_4$ homoclinic intersections in the right-well alone and in the left-well alone respectively occur. These two regions are due to the asymmetry in the potentials. For $\alpha$, $f > 0$ the area of the region $R_4$ is much smaller than the other regions. However, the area of $R_4$ in system-3 is much larger than those of systems 1 and 2.
- In systems 1 and 2, $f_M^{-} = f_M^{+}$ at a value of $\alpha$, say $\alpha'$, in addition to the value $\alpha = 1$ (figures 2a and 2b) and there are two $R_3$ regions, one with $\alpha < \alpha'$ and the other with $\alpha > 1$. In system-3, the regions $R_1 - R_4$ occur only once and all these regions meet at the point ($\alpha = 1$, $f = f_M^{+} = f_M^{-}$) which corresponds to the symmetrical system.
- In systems 1 and 2, for $\alpha < \alpha'$ and $\alpha > 1$, we find $f_M^{+} < f_M^{-}$ while $f_M^{+} > f_M^{-}$ for $\alpha' < \alpha < 1$. In system-3 $f_M^{+} > f_M^{-}$ for $\alpha < 1$ while $f_M^{+} < f_M^{-}$ for $\alpha > 1$.

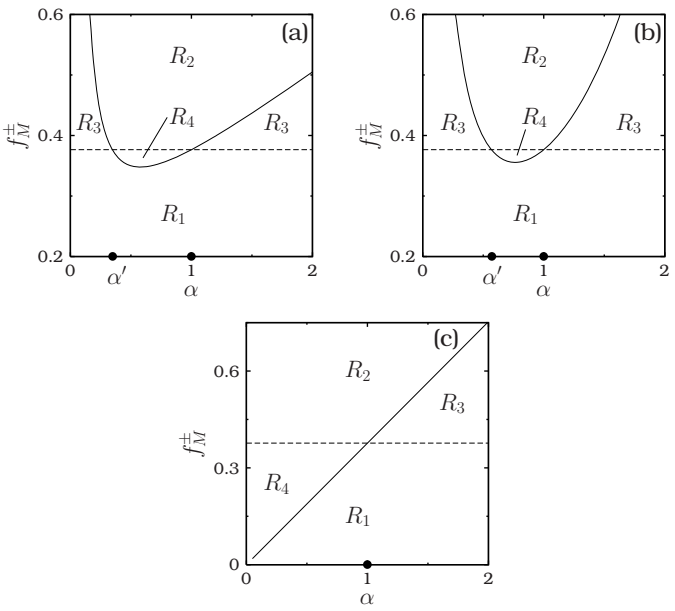


**Figure 2.** Plots of $f_M^+$ and $f_M^-$ vs. $\alpha$ for (**a**) system-1, (**b**) system-2 and (**c**) system-3. In all the subplots dashed horizontal line and continuous curve represent $f_M^+$ and $f_M^-$ respectively. The two closed circles in the subplots (**a**) and (**b**) for systems 1 and 2 mark the values of $\alpha$, namely $\alpha'$ and 1, at which $f_M^- = f_M^+$. For system-3, $f_M^- = f_M^+$ only at $\alpha = 1$.

Next, we fix the value of $\alpha$ and vary the frequency $\omega$ of the driving force. The threshold curves in $(f, \omega)$ plane have certain similarities and differences with those in the $(\alpha, f)$ plane:

- In all the three systems the threshold curves are nonlinear (figure 3).
- For systems 1 and 2 the $f_{\mathrm{M}}^-$ curve for a fixed value of $\alpha$ crosses $f_M^+$ curve and the $(f, \omega)$ plane can be divided into four regions similar to those noticed in the $(\alpha, f)$ plane. For system-3, for each value of $\alpha$, the $f_M^-$ and $f_M^+$ curves are noncrossing and they divide the $(f, \omega)$ plane into three regions only.
- For systems 1 and 2 for each value of $\alpha$ there exists a critical frequency $\omega_{\mathrm{c}}$ at which $f_M^- = f_M^+$. However, in system-1, as $\alpha$ increases $\omega_{\mathrm{c}}$ also increases while in system-2, $\omega_{\mathrm{c}}$ decreases with increase in $\alpha$. In system-3, for each value of $\alpha$, $\alpha \neq 1$, $f_M^-$ is always different from $f_M^+$.
- Consider system-3. From figure 3c we infer that for $\alpha < 1$ occurrence of the right-well homoclinic bifurcation alone cannot be observed for any set of values of $(f, \omega)$. Similarly, for $\alpha > 1$ the left-well homoclinic intersection alone is not possible. These two properties of system-3 in $(f, \omega)$ plane are not found in $(\alpha, f)$ plane for the other two systems.

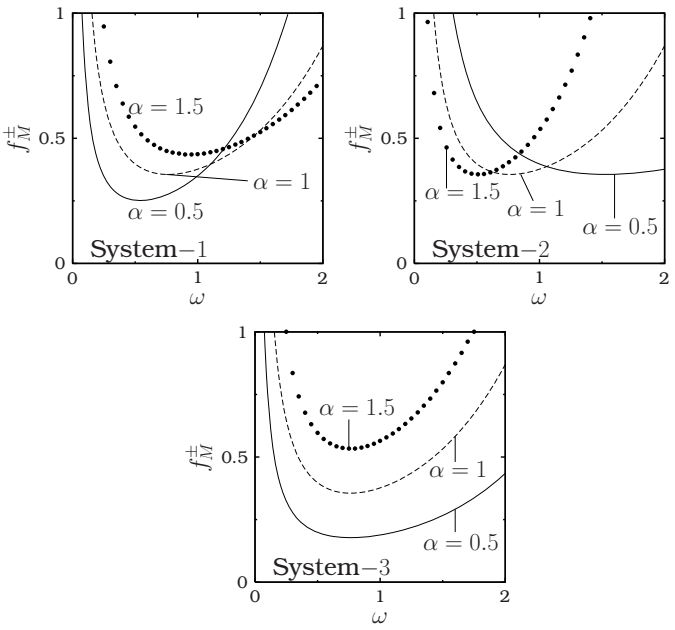


**Figure 3.** Melnikov threshold curves for homoclinic intersections in $(f, \omega)$ parameter plane for fixed values of $\alpha$ for the three asymmetrical systems. In all the subplots the dashed curve represents $f_M^+$ (as well as $f_M^-$ for $\alpha = 1$).

## 3. Numerical results

In this section we numerically integrate the equations of motion of the three asymmetrical systems and verify the analytical results obtained from the Melnikov function.

First, we show an example in system-1 where, when $f$ is varied transverse intersection of manifolds of the saddle in the right-well alone is not possible but other cases are possible. This happens when $f_M^- < f_M^+$. For $\alpha = 0.5$ we find $f_M^- = 0.345$ and $f_M^+ = 0.3765$. No intersection of stable and unstable parts of $W^-$ and $W^+$ occur for $f < f_M^-$ (figure 4a); left homoclinic intersections of $W_{\rm u}^-$ and $W_{\rm s}^-$ alone occur for $0.345 < f < 0.3765$ (figure 4b) and transverse intersections of both the left-well and the right-well orbits occur for $f > 0.3765$ (figure 4c).

In order to know the nature of local bifurcations near the Melnikov threshold values, we numerically study the long time motion. Figures 5a and 5b show two bifurcation diagrams, one with the initial condition chosen in the left-well and the other with the initial condition chosen in the right-well for the starting value of $f$. In the left-well, at $f = 0.3556$ (which is close to the Melnikov threshold value $f_M^- = 0.345$), the period-$2T$ orbit becomes unstable and the trajectories with various initial conditions jump to the right-well after a long transient and remains there forever. At $f = 0.365$ the chaotic attractor which is previously confined to the right-well now begins to visit the left-well also. Initially the orbit visits only

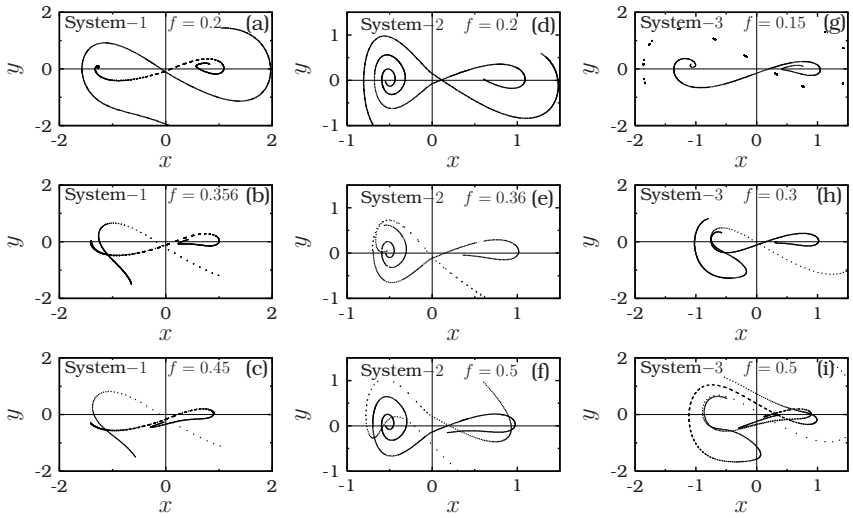


**Figure 4.** Stable and unstable manifolds of the saddle of systems 1, 2 and 3 for three values of $f$. $\alpha = 0.5$ for systems 1 and 3 and is 0.75 for system-2. The subplots (**a**–**c**), (**d**–**f**) and (**g**–**i**) are for systems 1, 2 and 3 respectively.

a small region near the origin in the left-well. At $f = 0.3835$ the onset of fully cross-well chaotic motion (crossing both the minima of the wells) is found. This value of $f$ is close to the analytically predicted Melnikov critical value $f_M^+ = 0.3765$.

For system-2 with $\alpha = 0.75$ we find $f_M^- = 0.3557$ and $f_M^+ = 0.3765$. Transverse intersection of homoclinic orbits do not occur for $0 < f < f_M^- = 0.3557$. Intersections of stable and unstable orbits in the left-well alone can occur for $0.3557 < f < 0.3765$. For $f > 0.3765$ orbits in the two wells can intersect. These are shown in figures 4d–4f. Similar dynamics is found in system-3 also. For example, when $\alpha = 0.5$ the Melnikov threshold values are $f_M^- = 0.1883$ and $f_M^+ = 0.3765$. As shown in figure 4g for $f = 0.15 < f_M^-$ the stable and unstable parts of $W^+$ and $W^-$ are well separated; at $f = 0.3$ (figure 4h) which lies between $(f_M^-, f_M^+)$ transverse intersections of the left-well manifolds alone occur and for $f = 0.5 > f_M^+$ (figure 4i) the stable and unstable parts of both $W^+$ and $W^-$ intersect. Dynamics highly sensitive to initial conditions chosen in the left-well is observed near $f_M^- = 0.1883$. At $f = 0.192$, after a chaotic transient, the trajectories from the left-well jump to the right-well and settle to a period-$T$ $(= 2\pi/\omega)$ attractor confined to the right-well. Cross-well chaotic motion occurs at $f = 0.3835$.

For a range of fixed values of $\alpha$, systems 1, 2 and 3 have $f_M^- > f_M^+$. In this case, when $f$ is varied from a small value, we have the scenario of no transverse intersection of stable and unstable parts of $W^+$ and $W^-$ for $0 < f < f_M^+$; transverse intersections of the manifolds $W_{\rm s}^+$ and $W_{\rm u}^+$ in the right-well alone for $f_M^+ < f < f_M^-$ and intersections of the stable and unstable parts of $W^+$ and $W^-$ in the two wells for $f > f_M^-$. For example, for system-2 with $\alpha = 1.5$ the Melnikov threshold values are $f_M^+ = 0.3765$ and $f_M^- = 0.533$. Figure 6 shows the numerically computed stable and unstable manifolds of homoclinic orbits for three values of $f$. In figure 6b

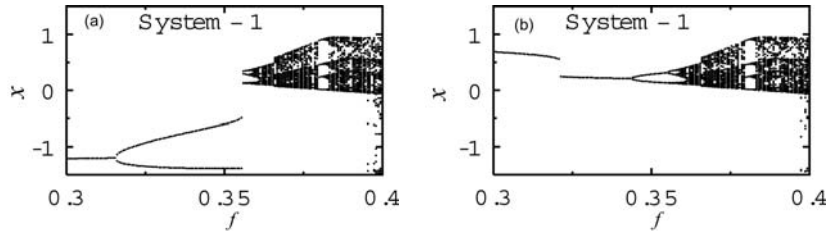


**Figure 5.** Bifurcation diagrams of system-1 with the initial condition chosen in the left-well (**a**) and in the right-well (**b**) for the starting value of $f$ for $\alpha = 0.5$.

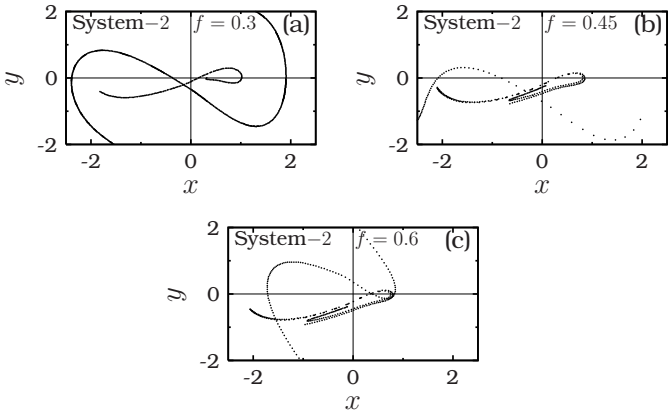


**Figure 6.** Numerically computed part of the stable and unstable manifolds of homoclinic orbits in the Poincaré map of system-2 for three values of $f$ for $\alpha = 1.5$.

where $f = 0.45$ lying between $f_M^+$ and $f_M^-$ intersections of the stable and unstable parts of $W^+$ alone are seen. For $f = 0.6$ intersection greater than $f_M^+$ and $f_M^-$ of stable and unstable parts of both $W^+$ and $W^-$ are noticed (figure 6c). The onset of chaotic motion confined to the right-well is found at $f = 0.3588$ which is close to the analytical threshold value $f_M^+ = 0.3765$. At $f = 0.54$, a value of $f$ close to $f_M^- = 0.533$ cross-well chaotic motion is observed. Similar results are found for systems 1 and 3.

We note that for $\alpha = 1$ there is no parametric values for which no attractor exists in the left-well or right-well. When $\alpha \neq 1$ in the three systems depending upon the values of $\alpha$ there are regions in the parameter space where there is no attractor in the left-well or in the right-well. For a range of values of $f$ the equations of motion of the systems 1–3 are numerically integrated for $10^4$ initial conditions chosen in the interval $x$, $\dot{x} \in [-2, 2]$. For each initial condition, we found the attractor after leaving 500 drive cycles as transient. Based on this analysis and the phase portrait of the attractors we numerically identified the range of values of $f$ where no attractor exists in the left-well or right-well. For $\alpha = 0.5$ there is no attractor in the region $x < 0$ in systems 1 and 3 for $f \in [0.356, 0.365]$ and $f \in [0.2, 0.365]$ respectively. On the other hand, when $\alpha = 1.5$ attractor is not found in the region $x > 0$ in systems

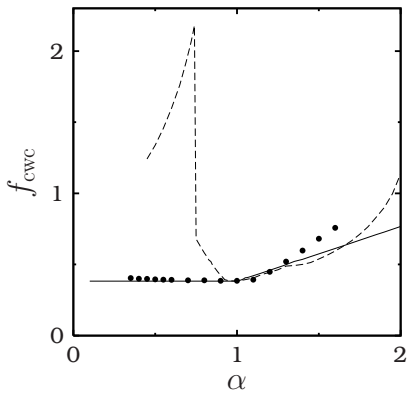


**Figure 7.** Plot of $f_{\rm cwc}$ (onset of cross-well chaos) as a function of $\alpha$ for three asymmetrical systems. The $f_{\rm cwc}$ of systems 1, 2 and 3 are represented by closed circles, dashed line and continuous line respectively.

1 and 3 for $f \in [0.38, 0.67]$ and $f \in [0.383, 0.55]$ respectively. In system-2, for both $0 < \alpha < 1$ and $\alpha > 1$, attractor confined to the region $x > 0$ or partly visiting it is not found for a range of values of the control parameter $f$. For example, for $\alpha = 0.5$ and 1.5 there is no attractor in the right-well for $f \in [0.365, 0.58]$ and $f \in [0.4, 0.52]$ respectively. Thus, by tuning the parameters it is possible to make all the trajectories to be confined in the region $x < 0$ or $x > 0$.

For a range of values of $\alpha$ we have calculated the critical value of $f$, $f_{\rm cwc}$, at which the onset of cross-well chaos occurs in the three asymmetrical systems. Figure 7 shows the variation of $f_{\rm cwc}$ as a function of $\alpha$ in the three systems.

## 4. Conclusion

We considered a linearly damped and periodically driven Duffing oscillator with three asymmetrical double-well potentials. Both analytically and numerically the occurrence of horseshoe chaos is studied. For the symmetrical Duffing oscillator system $f_M^- = f_M^+$ and the parameter space is divided into two regions by the Melnikov threshold curve. In contrast, in the three asymmetrical systems two additional regions where intersections of the left-well orbits alone and the right-well orbits alone occur do also exist. For a certain range of values of the control parameters there is no attractor in the left-well or in the right-well. This possibility is also not found in the symmetrical system. Furthermore, it would be important to analyse the effect of asymmetry on nonlinear phenomena such as stochastic and vibrational resonances in multi-well oscillators [25–27].

## Acknowledgement

The work of SR forms part of a Department of Science and Technology, Government of India sponsored research project. MAFS acknowledges financial support from the Spanish Ministry of Education and Science under project number FIS2006-08525.

## References


[1] M Lakshmanan and S Rajasekar, *Nonlinear dynamics: Integrability, chaos and patterns* (Springer, Berlin, 2003)
[2] E Simiu, *Chaotic transitions in deterministic and stochastic dynamical systems* (Princeton University Press, New Jersey, 2002)
[3] V Ravichandran, V Chinnathambi and S Rajasekar, *Phys.* **A376**, 223 (2007) and references therein
[4] R Räty, J von Boehm and H M Isomaki, *Phys. Rev.* **A34**, 4310 (1986)
[5] G Cicogna and F Papoff, *Europhys. Lett.* **3**, 963 (1987)
[6] M Arrayas, M I Dykman, R Mannella, P V E McClintock and N D Stein, *Phys. Rev. Lett.* **84**, 5470 (2000)
[7] S Lenci and G Rega, *Nonlin. Dyn.* **33**, 71 (2003)
[8] S Lenci and G Rega, *Chaos, Solitons and Fractals* **21**, 1031 (2004)
[9] H Cao, J M Seoane and M A F Sanjuán, *Chaos, Solitons and Fractals* **34**, 197 (2007)
[10] F Balibrea, R Chacon and M A Lopez, *Chaos, Solitons and Fractals* **24**, 459 (2005)
[11] A Litvak-Hinenzon and V Rom-Kedar, *Phys. Rev.* **E55**, 4964 (1997)
[12] C S Wang, Y H Kao, J C Huang and Y S Gou, *Phys. Rev.* **A45**, 3471 (1992)
[13] J A Almendral, J Seoane and M A F Sanjuán, *Recent Res. Devel. Sound Vib.* **2**, 115 (2004)
[14] J A Almendral and M A F Sanjuán, *J. Phys.* **A36**, 695 (2003)
[15] V Ravichandran, V Chinnathambi and S Rajasekar (2009) submitted for publication
[16] R Chacon, *Phys. Rev.* **E54**, 6153 (1996)
[17] R Chacon and J D Bejarno, *Phys. Rev. Lett.* **71**, 3103 (1993)
[18] M A F Sanjuán, *Int. J. Bifurcat. Chaos* **9**, 735 (1999)
[19] M S Siewe, H Cao and M A F Sanjuán, *Chaos, Solitons and Fractals* (2009), in press
[20] J Guckenheimer and P Holmes, *Nonlinear oscillations, dynamical systems and bifurcations of vector fields* (Springer, New York, 1983)
[21] K Chun and N O Birge, *Phys. Rev.* **B48**, 11500 (1993)
[22] N M Zimmerman *et al*, *Phys. Rev. Lett.* **67**, 1322 (1991)
[23] R Lofstedt and S N Coppersmith, *Phys. Rev. Lett.* **72**, 1947 (1994)
[24] S Wiggins, *Introduction to applied nonlinear dynamical systems and chaos* (Springer, New York, 1990)
[25] M S Siewe and F M Moukam Kakmeni, C Tchawoua and W Woafo, *Physica* **A357**, 383 (2005)
[26] Z Jing, Z Yang and T Jiang, *Chaos, Solitons and Fractals* **27**, 722 (2006)
[27] R Bourkha and M Belhaq, *Chaos, Solitons and Fractals* **34**, 621 (2007)